JOURNAL OF SPACECRAFT AND ROCKETS
Vol. 44, No. 5, September–October 2007

Interplanetary Mission Design Using Differential Evolution

Aaron D. Olds* and Craig A. Kluever†
University of Missouri–Columbia, Columbia, Missouri 65211
and
Michael L. Cupples‡
Science Applications International Corporation, Huntsville, Alabama 35806

DOI: 10.2514/1.27242

Global optimization methods have been increasingly under consideration for preliminary interplanetary mission design. One promising global method, differential evolution, has been identified as being particularly well suited to high-thrust trajectory optimization. Differential evolution is a stochastic direct search optimization method which uses parameter vectors that interact in a manner motivated by the evolution of living species. To improve the performance of differential evolution for this application, the effect of the tuning parameters is investigated over a diverse group of trajectory optimization problems. The quality of solutions obtained with differential evolution is found to be very sensitive to the selection of the routine's tuning parameters. A set of tuning parameter values is found that results in the rapid global optimization of an array of typical ballistic interplanetary missions. The fine-tuned differential evolution routine is implemented in a new tool, the mission-direct trajectory optimization program, and the effectiveness of this tool is demonstrated by the rapid solution of interplanetary trajectory optimization problems that involve complex features such as multiple gravity assists and parking orbit considerations.

Nomenclature

a	=	semimajor axis, km
CR	=	crossover probability
C_3	=	launch energy, km^2/s^2
E	=	orbital energy, km^2/s^2
e	=	eccentricity
F	=	mutation constant
i	=	inclination, rad
NP	=	population size
P_s	=	probability of obtaining a particular solution in one trial
r	=	radius, km
$\boldsymbol{r}_p$	=	periapsis vector, km
r_p	=	periapsis radius, km
T_{trial}	=	real-time run time of single DE trial, min
$T_{95\%}$	=	real-time run time required to find an optimum solution with 95% confidence, min
$\boldsymbol{u}$	=	trial vector
V	=	velocity, km/s
$\boldsymbol{V}_\infty$	=	hyperbolic excess velocity vector, km/s
V_∞	=	hyperbolic excess speed, km/s
$\boldsymbol{v}$	=	mutant vector
$\boldsymbol{x}$	=	target vector
ΔV	=	impulsive change in velocity, km/s
δ	=	flyby turn angle, rad
η	=	angle between incoming hyperbola asymptote and periapsis vector, rad
θ	=	B-plane angle, rad
μ	=	gravitational parameter, km^3/s^2
φ_{Lat}	=	landing site latitude, rad
Ω	=	right ascension of ascending node, rad
ω	=	argument of periapsis, rad

Subscripts

allow	=	allowable
EI	=	entry interface
G	=	generation number
GA	=	gravity assist
hyp	=	hyperbola
min	=	minimum
PO	=	parking orbit
req	=	required
up	=	unpowered
α	=	right ascension
δ	=	declination

Superscripts

$+$	=	outgoing
$-$	=	incoming

Introduction

THE use of global optimization routines for interplanetary missions is driven by the desire to quickly, and with minimal effort, locate the best solution to complicated trajectory optimization problems. Compared to the use of local optimization techniques, which require the user to initially locate the basin of attraction of the best solution, global methods search over the entire design space and find the best solution without a priori knowledge of its location. A global method has the advantage of eliminating a large portion of user interaction, which, with the high power of contemporary computers, can substantially reduce the time invested in solving difficult optimization problems.

Global optimization techniques have often been applied to trajectory optimization problems. Hartman et al. [1] and Crain et al. [2] applied genetic algorithms to produce a good initial guess for local gradient-based optimization methods. These techniques were applied to low-thrust interplanetary transfers in [1] and ballistic interplanetary transfers in [2], respectively. Vasile and De Pascale [3]

Presented as Paper 155 at the 16th AAS/AIAA Space Flight Mechanics Meeting, Tampa, FL, 22–26 January 2006; received 11 August 2006; revision received 20 April 2007; accepted for publication 28 April 2007.

*Graduate Student, Mechanical and Aerospace Engineering Department, currently Project Engineer, Analytical Mechanics Associates, Hampton, VA 23666; Olds@ama-inc.com. Member AIAA.

†Professor, Mechanical and Aerospace Engineering Department; KlueverC@missouri.edu. Associate Fellow AIAA.

‡Systems Engineer, In-Space Technology Assessment Lead, 6725 Odyssey Drive; currently Systems Engineer, Raytheon Missile Systems, 1151 East Hermans Road, Tucson, AZ 85706; Michael_Cupples@raytheon.com.

developed a global search method with a systematic branching strategy and used this approach to successfully obtain optimal interplanetary missions with multiple gravity assists. Bessette and Spencer [4] compared the performance of various global search methods by solving a standard orbital transfer problem.

Recent work, such as [4], suggests that determining which particular global search method is most appropriate for trajectory optimization is still a debatable issue. For example, selecting the "best" global optimization routine for ballistic trajectory design was the topic of two recent ESA-funded studies contracted to the University of Reading [5] and the University of Glasgow [6]. The University of Reading study concluded that differential evolution (DE) was the best global search method for use with multiple gravity-assist trajectories with deep space maneuvers (DSM). The set of global routines that were investigated in the Reading study include divided rectangles (DIRECT), multilevel coordinated search (MCS), probabilistic global search Lausanne (PGSL), cross entropy (CE), simple genetic algorithm (GA), particle swarm optimization (PSO), multiple particle swarm optimization (MPSO), and DE. The University of Glasgow study found DE to have only average performance relative to other routines investigated, which included genetic algorithm for optimization toolbox (GAOT), GAOToolbox with sharing operator (GAOT-shared), genetic algorithm toolbox (GATBX), genetic algorithm toolbox with migration operator (GATBX-migr), fast evolutionary programming (FEP), DE, adaptive simulated annealing (ASA), global solver (GlbSolve), multilevel coordinated search (MCS), radial basis function solver (rbfSolve), and evolutionary predictive interval computation (EPIC). Both studies used a variation of the Cassini Mission profile without deep space maneuvers as one of the tests to rank the global optimization routines. This trajectory involves two Venus gravity assists, one Earth gravity assist, and one Jupiter gravity assist on the way from Earth to Saturn. For this problem, the University of Reading analysis found, after 20 DE runs, a minimum total ΔV of 6142 m/s and a mean value of 8419 m/s. The best known solution from running all global search methods was a total ΔV of 6142 m/s. The Glasgow study ran DE 10 times and found a minimum total ΔV of 7511 m/s and a mean value of 10, 145 m/s. The smallest known total ΔV from running all global search methods was 6368 m/s, which differs from the best solution in the Reading report due to slight differences in the problem definition.

One possible explanation for the better results for DE in the Reading study is the inconsistency of the DE tuning parameter set compared to the tuning parameters used in the Glasgow report. Differential evolution has three basic parameters that may be modified to alter the algorithm's behavior: the population size NP, the crossover probability CR, and the mutation scaling factor F (these tuning parameters will be discussed in detail in a later section). Therefore, based on these two ESA studies, it appears that the performance of a leading global search candidate such as DE heavily depends on properly selecting these stochastic tuning parameters.

In this paper, the relationship between DE's performance and its tuning parameter values is systematically investigated over a diverse group of test problems. The objective is to identify the best set for use with any ballistic interplanetary trajectory optimization problem. To implement differential evolution, a new trajectory optimization tool, the mission-direct trajectory optimization program (MDTOP), is developed, which is designed to perform end-to-end preliminary design of high-thrust missions [7]. Numerical solutions are presented for four complex interplanetary missions to demonstrate the effectiveness of coupling MDTOP with a well-tuned DE algorithm.

Solar System Model

For preliminary mission design, it is important that the solar system model allows alternative trajectories to be compared so that an optimum solution can be found. It is desirable that the model allows the performance of a mission be analyzed as quickly as possible, while yielding an accurate approximation of the time and propulsion required to complete the mission. It is not as important to have high positional accuracy, as absolute position is very sensitive to small propulsive maneuvers. For these reasons, a linked conic, zero sphere-of-influence model of the solar system is used. This means that for the interplanetary legs of a mission the sun is the only attracting body. For operations that take place near a planet such as arrival, departure, or flyby, the planet is assumed to be the only attracting body. Heliocentric trajectory legs terminate at the locations of the planets with a velocity $\boldsymbol{V}_\infty$ relative to the planet. Planetocentric trajectories are assumed to begin and/or end at an infinite distance from the planet, with a hyperbolic excess velocity equal to $\boldsymbol{V}_\infty$. These simplifications place the spacecraft in a two-body gravity field at all times, which allows for fast computation.

One key component of interplanetary trajectory analysis is the ability to know a spacecraft's heliocentric state vector (position and velocity) at any time during a mission. Only the initial state, $\mathbf{r}(T_1)$ and $\mathbf{v}(T_1)$, and the final state, $\mathbf{r}(T_2)$ and $\mathbf{v}(T_2)$, need to be known, because no propellant is used while the spacecraft coasts on conic trajectories. This problem does not have a closed-form solution, but it can be solved iteratively using one of two popular formulations, Kepler's problem and the Gauss/Lambert problem. The Gauss/Lambert problem is used by MDTOP because it yields an optimization problem that inherently satisfies position matching constraints between the ends of interplanetary trajectory legs. A universal variable formulation of the Lambert problem is used to solve for the spacecraft state vectors [8]. The direction of motion for the transfer, DM, is analytically determined such that all trajectories are prograde with respect to the planets' orbital velocities. A formulation of the Gauss/Lambert problem is

$$\text{given: } \mathbf{r}(T_1), \mathbf{r}(T_2), DM \qquad \text{find: } \mathbf{v}(T_1), \mathbf{v}(T_2) \tag{1}$$

The planets' positions are determined as a function of time from static ephemerides. Static ephemerides are used for the results documented in this study in lieu of more accurate ephemeris gererators such as Jet Propulsion Laboratory (JPL)'s DE405 due to the associated run-time savings. Once the heliocentric trajectory legs have been solved for using Lambert's theorem, the planetocentric operation details are calculated from the $\boldsymbol{V}_\infty$ vectors that result. There are five supported operations that can take place within the planets' sphere of influence: planetary flyby, departure from a parking orbit, arrival into a parking orbit, atmospheric entry, and ground based launch. Each of these cases can be easily analyzed if all points on a trajectory are confined to a plane. This is a reasonable condition, due to the large amount of energy required to perform out-of-plane maneuvers. A planetocentric orbital plane is allowed to have any orientation as long as it includes $\boldsymbol{V}_\infty$.

By making use of gravity assists at intermediate planets in a trajectory, the propellant requirements for a mission can be dramatically reduced. For the purposes of preliminary trajectory optimization, the turn angle δ characterizes the maneuver, and can be calculated from [9]

$$\delta = 2\sin^{-1}\left(\left[1 + \frac{2r_p V_\infty^{-2}(Er_p + \mu)}{\mu^2}\right]^{-1/2}\right) \tag{2}$$

For an unpowered flyby, energy E is conserved, which implies that the magnitude of incoming velocity at infinity V_∞^- is equal to the magnitude of the outgoing velocity at infinity V_∞^+. Therefore, the geometry of the flyby is determined only by the plane of the trajectory, the gravitational parameter of the planet μ, the closest approach distance r_p, and the hyperbolic excess speed V_∞^-.

When flybys are used to connect two heliocentric trajectories at a planet (as is the case when the Lambert formulation is used) the geometry of the flyby can be analytically determined from the incoming hyperbolic excess velocity $\boldsymbol{V}_\infty^-$ and the outgoing hyperbolic excess velocity $\boldsymbol{V}_\infty^+$ when the scalar V_∞^- is not necessarily equal to V_∞^+. The first step in the process is to determine the flyby plane from the cross product of the incoming and outgoing $\boldsymbol{V}_\infty$ vectors. Next, the angle between the $\boldsymbol{V}_\infty$ vectors, δ_{req}, is calculated. The minimum allowable periapsis radius $r_{p,\min}$ is used to find the largest allowable turn angle δ_{allow}, by substitution into Eq. (2). Then, $\boldsymbol{V}_\infty^-$ is rotated in the flyby plane by the smaller value of δ_{req} and δ_{allow}

to produce $\boldsymbol{V}^+_{\infty,\mathrm{up}}$, the unpowered outgoing $\boldsymbol{V}_\infty$ vector. $\boldsymbol{V}^+_{\infty,\mathrm{up}}$ is then compared with the required $\boldsymbol{V}^+_\infty$ via Eq. (3) to determine any required ΔV at "infinity" to match the initial heliocentric velocity of the next trajectory leg:

$$\Delta V_{\mathrm{GA}} = \|\boldsymbol{V}^+_\infty - \boldsymbol{V}^+_{\infty,\mathrm{up}}\| \tag{3}$$

In general, flybys are powered, with an unpowered flyby being the special case when $\boldsymbol{V}^+_{\infty,\mathrm{up}}$ equals $\boldsymbol{V}^+_\infty$.

A common end condition for a mission is the use of parking orbits for arrival or departure at a planet. Parking orbits are often used as staging areas before descent to, or after ascent from, the surface. If the plane of the parking orbit is known, and the transfer between the incoming or outgoing hyperbola is coplanar with the parking orbit and tangent to periapsis, then the required impulsive velocity change ΔV_{PO}, required to complete the transfer, can be obtained from

$$\Delta V_{\mathrm{PO}} = \sqrt{V^2_\infty + \frac{2\mu}{a(1-e)}} - \sqrt{\frac{(1+e)\mu}{(1-e)a}} \tag{4}$$

All that is required to be known to calculate the ΔV is the semimajor axis a and eccentricity e of the parking orbit, and the hyperbolic excess speed V_∞ from the heliocentric trajectory.

Another type of end condition occurs when the periapsis radius of the incoming hyperbola is less than the radius of the planet's sensible atmosphere r_{EI}. In this case, the spacecraft arrives at the planet's entry interface at a speed V_{EI}, which can be calculated in a two-body gravity field by

$$V_{\mathrm{EI}} = \sqrt{V^2_\infty + \frac{2\mu}{r_{\mathrm{EI}}}} \tag{5}$$

Because of the large forces and heating rates associated with fast atmospheric entries, an upper limit on entry interface speed is often imposed.

The use of Eq. (4) for determining the ΔV involved in a transfer into or out of a parking orbit only applies if the planetocentric hyperbola that results from the interplanetary trajectory is in the same plane with and shares a common periapsis location with the desired parking orbit. That orbital geometry is only a special case and the general use of Eq. (4) may result in overly optimistic mission performance predictions [10]. The next section presents the approach used in MDTOP for including realistic parking orbit requirements in the optimization of a round-trip surface mission with orbital rendezvous.

Round-Trip Parking Orbit Determination

The global nature of the DE algorithm allows for parking orbits to be easily included as part of the overall trajectory optimization. An example of a direct, round-trip, surface mission to Mars that includes rendezvous with the return stage in orbit illustrates the approach used to model parking orbit operations. To obtain the most efficient descent to the planet's surface, periapsis is constrained to lie directly above the landing site. Taking advantage of Mars' atmospheric drag to slow the spacecraft, the only significant propulsive action necessary to land on the planet is to enter the atmosphere with an in-plane, minimum-energy, 180-deg transfer from the apoapsis of the arrival parking orbit. For ascent back to the parking orbit, the atmosphere provides no advantage, so the location of periapsis is modeled to be independent of the landing site, though the orbit inclination must exceed the landing site latitude for an in-plane ascent to be possible.

A number of further assumptions are involved in this orbital rendezvous model. First, only natural perturbations due to the planet's oblateness, J_2 effects, are allowed to align the parking orbit with the departure hyperbola. Second, the burns for insertion into and injection out of the parking orbit are assumed to occur at periapsis and to be tangential to the parking orbit. Third, the planet is assumed to be rotating at a high rate relative to its rate of revolution about the sun. This allows for landing site latitude to be specified instead of the more restrictive latitude and longitude of a physical landing site. It is assumed that the cost in propulsion is negligible to arrive a few hours before or after the optimal time, to achieve the correct landing site longitude.

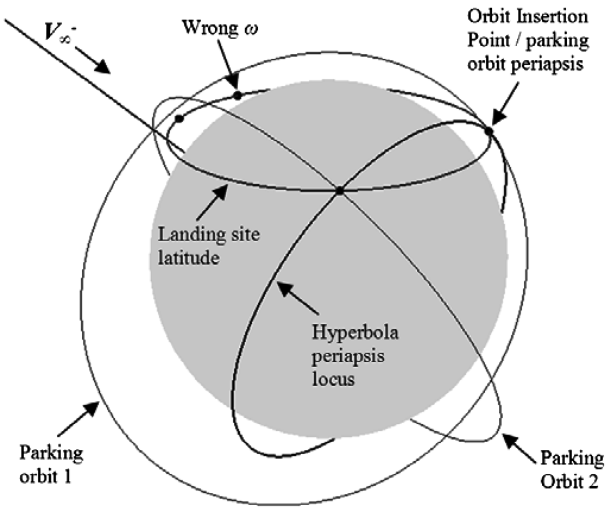

Fig. 1 Orbital insertion geometry.

For any incoming hyperbola that meets all the following criteria

$$\left\{\begin{array}{l} V_{\infty,\delta} - \eta + \pi \geq \varphi_{\mathrm{Lat}} \\ V_{\infty,\delta} + \eta - \pi \leq \varphi_{\mathrm{Lat}} \\ V_{\infty,\delta} - \eta \leq -\varphi_{\mathrm{Lat}} \\ V_{\infty,\delta} + \eta \geq -\varphi_{\mathrm{Lat}} \end{array}\right\} \tag{6}$$

the locus of possible hyperbola periapsis locations intersects the desired landing site latitude. These criteria ensure that two parking orbits exist which have a common periapsis with the incoming hyperbola at the latitude of the landing site as illustrated in Fig. 1. In Eq. (6), η is the angle between the incoming $\boldsymbol{V}_\infty$ vector and the hyperbola's periapsis vector, and is calculated by

$$\eta = \cos^{-1}\left(\frac{-1}{e}\right) \tag{7}$$

The symbol $V_{\infty,\delta}$ is the declination of the incoming $\boldsymbol{V}_\infty$ vector. In the aim-point coordinate frame, the angle θ defines the plane of the incoming hyperbola. The two possible arrival parking orbits, if they exist, lie on their respective planes defined by θ_1 and θ_2. Based upon spherical geometry, θ_1 can be obtained from

$$\theta_1 = \left\{\begin{array}{ll} -\sin^{-1}\left(\frac{\sin^2(\varphi_{\mathrm{Lat}})}{\sqrt{\cos^2(V_{\infty,\delta})\sin^2(\eta)\sin^2(\varphi_{\mathrm{Lat}})}} + \frac{\tan(V_{\infty,\delta})}{\tan(\eta)}\right), & \varphi_{\mathrm{Lat}} \geq 0 \\ \sin^{-1}\left(\frac{\sin^2(\varphi_{\mathrm{Lat}})}{\sqrt{\cos^2(V_{\infty,\delta})\sin^2(\eta)\sin^2(\varphi_{\mathrm{Lat}})}} - \frac{\tan(V_{\infty,\delta})}{\tan(\eta)}\right), & \varphi_{\mathrm{Lat}} < 0 \end{array}\right. \tag{8}$$

such that the periapsis of the hyperbola lies at the landing site latitude. The plane defined by

$$\theta_2 = \pi - \theta_1 \tag{9}$$

shows the correlation between the two orbit planes and is the result of the symmetry of the problem.

The next step is to use θ_1 and θ_2 to obtain the orbital elements of the parking orbits which lie in the corresponding orbit planes and also share a common periapsis location with the incoming hyperbola. Equations (10–12) show how to obtain the inclination i, right ascension of the ascending node Ω, and argument of periapsis ω, for the arrival parking orbits which satisfy these conditions:

$$i = \cos^{-1}[\cos(\theta)\cos(V_{\infty,\delta})] \tag{10}$$

$$\Omega = \begin{cases} \sin^{-1}\left(\frac{\tan(V_{\infty,\delta})}{\tan(i)}\right) + V_{\infty,\alpha} - \pi, & \theta \geq \pi \\ -\sin^{-1}\left(\frac{\tan(V_{\infty,\delta})}{\tan(i)}\right) + V_{\infty,\alpha}, & \theta < \pi \end{cases} \tag{11}$$

$$\omega = \begin{cases} \sin^{-1}\left(\frac{\sin(\varphi_{\text{Lat}})}{\sin(i)}\right), & \text{if } (\boldsymbol{r}_{p,\text{PO}} = \boldsymbol{r}_{p,\text{hyp}}) \\ \pi - \sin^{-1}\left(\frac{\sin(\varphi_{\text{Lat}})}{\sin(i)}\right), & \text{if } (\boldsymbol{r}_{p,\text{PO}} = \boldsymbol{r}_{p,\text{hyp}}) \end{cases} \tag{12}$$

In these equations, $V_{\infty,\alpha}$ denotes the right ascension of the $\boldsymbol{V}_\infty$ vector. A parking orbit for in-plane descent, in general, will intersect the landing site latitude at two points. Equation (12) shows the two alternative values of ω that place the orbit's periapsis at the intersection points with the landing site latitude. Depending on the specific geometry of the scenario, one of the two arguments of periapsis will result in a parking orbit periapsis location that coincides with the incoming hyperbola periapsis location, allowing for tangential orbit insertion. The remaining ω refers to the other intersection of the landing site latitude with the orbit plane, as shown in Fig. 1, and is discarded. Equations (10–12) are used for both θ_1 and θ_2 to obtain the orbital elements of the two possible arrival parking orbits. The semimajor axis a and eccentricity e of the arrival parking orbits are design variables to be optimized.

For departure, the conditions placed upon the parking orbit are less stringent as the periapsis latitude is not required to coincide with the latitude of the landing site. Although the arrival orbit will precess during the surface stay, the inclination does not change. Therefore, the problem to be solved for the departure orbit is to find the ascending node Ω and the argument of periapsis ω, such that an orbit with specified inclination i lies in plane with the departure hyperbola and shares its periapsis location. Equations (13–16) are taken directly from the work of Desai and Buglia [11], and are used to define two orbits of the form: $[a, e, i, \Omega_1, \omega_1]$ and $[a, e, i, \Omega_2, \omega_2]$, which correspond to one of the two arrival parking orbit inclinations.

$$\Omega_1 = -\sin^{-1}\left(\frac{\tan(V_{\infty,\delta})}{\tan(i)}\right) + V_{\infty,\alpha} \tag{13}$$

$$\Omega_2 = \sin^{-1}\left(\frac{\tan(V_{\infty,\delta})}{\tan(i)}\right) + V_{\infty,\alpha} + \pi \tag{14}$$

$$\omega_1 = \sin^{-1}\left(\frac{\sin(V_{\infty,\delta})}{\sin(i)}\right) - \eta + \pi \tag{15}$$

$$\omega_2 = -\sin^{-1}\left(\frac{\sin(V_{\infty,\delta})}{\sin(i)}\right) - \eta + 2\pi \tag{16}$$

Because these equations are used for a departure orbit, the $\boldsymbol{V}_\infty$ vector in the following equations is actually equal to the negative of the $\boldsymbol{V}_\infty^+$ vector. Given $\boldsymbol{V}_\infty^+$ from the heliocentric trajectory and i_1 and i_2 from the two possible arrival parking orbits defined by Eq. (11), there exist four possible departure parking orbits, two corresponding to i_1 and two corresponding to i_2: $[a, e, i_1, \Omega_1, \omega_1]$, $[a, e, i_1, \Omega_2, \omega_2]$, $[a, e, i_2, \Omega_1, \omega_1]$, and $[a, e, i_2, \Omega_2, \omega_2]$. There are four possible combinations of precessed arrival parking orbits and departure parking orbits that may be used. The optimization proceeds by selecting the most closely matching precessed arrival orbit and departure orbit and penalizing the sum of the difference of their orbital elements.

For simplicity, the ascent and descent between the parking orbit and the surface are modeled as simple ballistic trajectories. The descent ΔV is calculated as the velocity change at the arrival orbit's apoapsis that is required to lower periapsis to the radius of the planet's sensible atmosphere. The ascent ΔV is calculated based upon the ideal change in energy necessary to transfer from the rotating planet's surface to the parking orbit directly overhead.

Differential Evolution

Differential evolution is a stochastic direct search method that uses a set of parameter vectors that interact in a way that is inspired by the evolution of living species [12]. Figure 2 shows a graphical representation of a DE population used for a simple trajectory optimization problem. In Fig. 2, each of the NP members of the population is named $\boldsymbol{x}_i$, where i is the member index. Each vector has D elements, where the jth element is the design variable index. The jth element corresponds to the same continuous design variable for each vector, though the value of the jth element can vary among the population.

DE initializes the population by assigning variable values from a uniform random distribution between the upper and lower limits of each variable. In each generation, the parameter vectors are modified to locate better solutions. DE uses three operations to spawn successive generations: mutation, crossover, and selection. The following process is repeated for each member of the current generation, $\boldsymbol{x}_{i,G}$. Three unique individuals are randomly chosen from the population: $\boldsymbol{x}_{r1,G}$, $\boldsymbol{x}_{r2,G}$, and $\boldsymbol{x}_{r3,G}$, where i, $r1$, $r2$, and $r3$ are different indexes. Next, a "differential variation" vector is generated by subtracting vector $\boldsymbol{x}_{r3,G}$ from vector $\boldsymbol{x}_{r2,G}$. This term is multiplied by a mutation scale factor F and added to $\boldsymbol{x}_{r1,G}$ to form a mutant vector $\boldsymbol{v}_{i,G+1}$. This process is called "mutation" and is mathematically described by

$$\boldsymbol{v}_{i,G+1} = \boldsymbol{x}_{r1,G} + F(\boldsymbol{x}_{r2,G} - \boldsymbol{x}_{r3,G}) \tag{17}$$

Following mutation, a process known as "crossover" takes place, which mixes the parameters of the target vector $\boldsymbol{x}_{i,G}$ and the mutant vector $\boldsymbol{v}_{i,G+1}$ to form a trial vector $\boldsymbol{u}_{i,G+1}$. A crossover constant, $CR \in [0, 1]$, is equivalent to the probability that a trial vector element will come from the mutant vector. For each of the D elements, a uniform random number rand$(j) \in [0, 1]$ is generated and compared with CR to determine if the jth value of $\boldsymbol{u}_{i,G+1}$ will come from $\boldsymbol{x}_{i,G}$ or $\boldsymbol{v}_{i,G+1}$. Figure 3 illustrates the crossover process.

After crossover, selection is the final operation. In selection, the better of the $\boldsymbol{u}_{i,G+1}$ and $\boldsymbol{x}_{i,G}$ vectors is chosen to survive to the next generation, $G + 1$. If $\boldsymbol{u}_{i,G+1}$ is a better solution than $\boldsymbol{x}_{i,G}$, then $\boldsymbol{u}_{i,G+1}$ will be assigned to $\boldsymbol{x}_{i,G+1}$ and $\boldsymbol{x}_{i,G}$ is discarded. Otherwise, $\boldsymbol{x}_{i,G}$

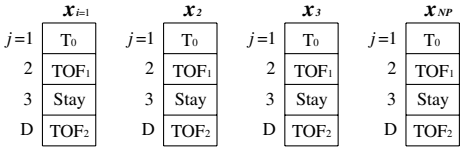

Fig. 2 Example population of parameter vectors.

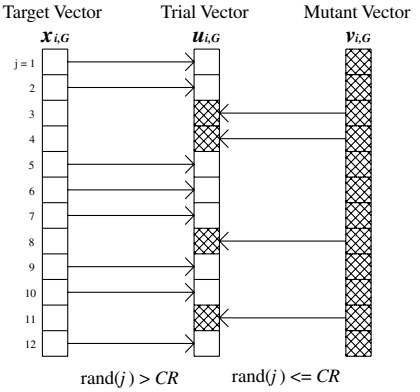

Fig. 3 Example of DE crossover operation to form trial vector.

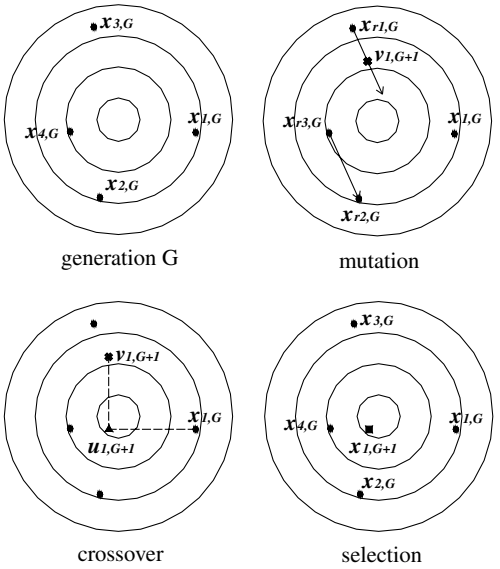

Fig. 4 Differential evolution operations on a single target vector.

moves into the next generation as $\boldsymbol{x}_{i,G+1}$ and $\boldsymbol{u}_{i,G+1}$ is discarded. For each generation, this process of mutation, crossover, and selection is repeated for all NP $\boldsymbol{x}_{i,G}$ vectors to form a new population of NP $\boldsymbol{x}_{i,G+1}$ vectors. The optimization continues until the prescribed number of generations is processed or until a termination condition is reached. Figure 4 illustrates the DE mechanism on a simple two-dimensional minimization problem. The design space here is a simple two-dimensional surface, with the best solution at the center. At the beginning of generation G, there are four parameter vectors, each consisting of two elements, one for the horizontal position in the design space and one for the vertical position. The mutation operation described by Eq. (17) is illustrated in the upper-right sketch. First, $\boldsymbol{x}_{i,G}$ is designated as the target vector. Randomly, each of the remaining three individuals is termed either $\boldsymbol{x}_{r1,G}$, $\boldsymbol{x}_{r2,G}$, or $\boldsymbol{x}_{r3,G}$. The position of $\boldsymbol{v}_{1,G+1}$ is generated as described by Eq. (17), with F in this case equal to 0.5. Crossover is undertaken with a CR value of 0.5. In Fig. 4 it can be seen that the trial vector $\boldsymbol{u}_{1,G+1}$ is composed of the horizontal, $j = 1$, position value of $\boldsymbol{v}_{1,G+1}$ and the vertical, $j = 2$, position value of $\boldsymbol{x}_{1,G}$. Because $\boldsymbol{u}_{1,G+1}$ is closer to the minimum than $\boldsymbol{x}_{1,G}$, the selection operation uses $\boldsymbol{u}_{1,G+1}$ to replace $\boldsymbol{x}_{1,G}$ in the next generation. Vector $\boldsymbol{x}_{1,G}$ will still be used as the remaining three parameter vectors take their turn as the target vector. Vector $\boldsymbol{x}_{1,G+1}$ is not used until the next generation.

To tailor DE to a particular problem, there are three parameters that may be varied: the population size NP, the mutation constant F, and the crossover probability CR. The optimization is terminated upon population convergence or when the maximum number of generations is reached, which, for the subsequent investigations, is set as the iteration number where progress is observed to have ceased for most runs. It should be noted that the DE scheme detailed here is of type *rand/1/bin*. This means that the vector to be mutated is selected at random, only one difference vector is used for mutation, and crossover is determined by independent binomial experiments. There are many other schemes in existence, though this is one of the most well known and the method used for all analyses in this study.

Tuning Parameter Analysis Method

To characterize the performance of the differential evolution routine in MDTOP, a test suite of four challenging interplanetary optimization problems is developed: the 1997 Cassini mission to Saturn, the 1989 Galileo mission to Jupiter, a comet Tempel 1 surface sample return mission, and a round-trip surface mission to Mars with orbital rendezvous. To test the generality of MDTOP, all four missions are optimized with the same set of bounds on the DSM location and trajectory leg time of flight. Deep space maneuvers are limited in this study to the region between the orbits of Earth and Jupiter within 5 deg of the ecliptic plane. Transfer times between inner planets are allowed to range from 0.1 to 1.5 orbital periods of the outermost planet involved. Resonate transfers that start and end at the same planet can range from 1:1 to 1:3 spacecraft revolutions to planet revolutions. Transfers that involve an outer planet can range in duration from 0.1 to 0.4 orbital periods of the outermost planet involved. The performance index used by DE to optimize the case studies is the total mission ΔV, neglecting velocity losses. Because no propulsion system performance information is involved in the analysis, no launch vehicle is specified. The goals of this investigation are to determine the time required to reliably locate the global optimum, and to identify an appropriate set of optimization tuning parameters for the diverse group of test missions.

Because DE relies on random operations to locate the global optimum, the solutions from a series of runs will, in general, not necessarily be the same. Therefore, any meaningful analysis of the results will be probabilistic in nature. The first step in comparing the results of alternative setups is to determine a suitable sample size. The Cassini mission to Saturn is assumed to be the most challenging optimization problem included in the study, and is therefore used to determine a sample size common to all analyses. The smallest sample size is selected which results in performance histograms that are practically identical. A standard set of 1000 trials was determined to be acceptable. Figure 5 shows two 1000-trial histograms for the optimized Cassini mission. To generate these two histograms, a population size of 20 is used with a crossover probability of 0.6, and a mutation coefficient of 0.4, for a maximum of 4000 generations.

Although the histograms are not identical, they are similar enough that all conclusions about one would also be made about the other. Some insights into the nature of the solutions obtained with DE can be obtained from just this one example. First, the method often

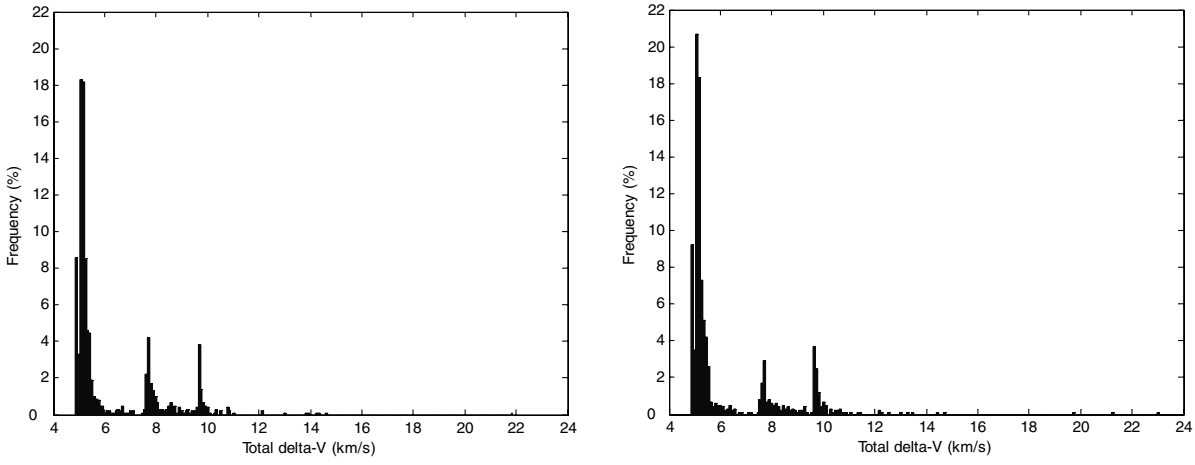

Fig. 5 Two 1000-trial histograms of the solutions for the Cassini mission profile.

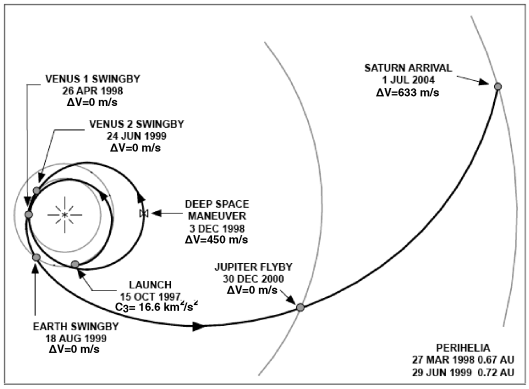

Fig. 6 Published trajectory for the Cassini mission [13].

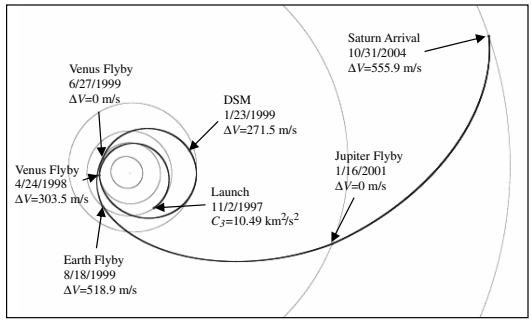

Fig. 7 Minimum ΔV solution obtained for Cassini mission profile with MDTOP.

converges to suboptimal minima. Second, the global minimum is not necessarily the most commonly found solution. The optimization routine may have to be run a number of times to find obscure global minima. Additionally, the user is not able to tell if the best solution found is actually the global minimum, as DE does not conduct an exhaustive search.

Total mission ΔV histograms are used to show the effect of the three DE optimization parameters, population size NP, crossover probability CR, and mutation coefficient F, on the quality of solutions obtained and the optimization time required. A meaningful performance index is developed to characterize alternative DE parameter setups. The performance index $T_{95\%}$ is selected to be equal to the actual computer run time required to find the best solution with a confidence level of 95%. Equation (18) defines the performance measure more precisely,

$$T_{95\%} = T_{\text{trial}} \frac{\log(1 - 0.95)}{\log(1 - P_S)} \tag{18}$$

where P_S is the probability of finding the minimum ΔV solution in one trial with MDTOP, which is equivalent to the vertical axis of the 1000 trial histograms. The value T_{Trial} is the average real run time for each optimization trial. All of the run times presented are obtained with a 3.0 GHz Pentium 4 processor. The range of total ΔV that is classified as belonging to the minimum ΔV solution is determined by an analysis of the solution space for each test case in order to calculate P_S. Additionally, the results are checked to ensure that only one solution occupies the minimum ΔV band. The best DE tuning parameters will result in short run times and a high probability of finding the global optimum, thereby minimizing $T_{95\%}$.

Because of the significant amount of time required to generate 1000 trial histograms for this analysis, the three-dimensional DE tuning parameter design space is discretized, with information from a brief initial investigation, into three population sizes NP: 20, 28, and 36; three crossover probabilities CR: 0.4, 0.6 and 0.8; and six mutation coefficients F: 0.2, 0.4, 0.6, 0.8, 1.0, and rand[−1, 1], where rand[−1, 1] is a uniformly distributed random mutation coefficient that is selected between −1 and 1 each generation. This results in 54 combinations under consideration for each of four case studies. To reduce the computing demands further, the 54 tuning parameter combinations are only run for the Cassini interplanetary trajectory, as it is assumed to be the most difficult of the four case studies. The best six parameter sets for Cassini are then compared over the remaining three test problems. The course discretization of the tuning parameters and the elimination of the majority of combinations after only one test problem mean that while this approach is designed to yield a high performing parameter set, it is not meant to find the best in existence.

Cassini Case Study

As one of the most complicated high-thrust interplanetary missions flown, Cassini serves as an excellent example to test the limits of differential evolution's performance. For the purpose of comparison, Fig. 6 shows the Cassini mission profile from [13]. For the optimization, 10 design variables are required: launch date, six times of flight for the six trajectory legs, and three variables to define the position of the deep space maneuver. The launch date is confined within the year 1997. The total mission duration is limited to seven years to approximately coincide with the time of flight of the Cassini mission, as longer times of flight are found to result in a lower total mission ΔV. The minimum flyby altitude of each planet is set at 300 km and the spacecraft enters a specified Saturn orbit with an altitude of 0.33×150 Saturn radii. The plane of the Saturn arrival orbit is undefined for this investigation. Figure 7 presents the minimum ΔV trajectory obtained by MDTOP for this mission profile.

A comparison of the event dates shows that the optimum MDTOP solution has some events very close to the Cassini dates, while others differ by many days. These differences are expected, as the physical model in MDTOP is the result of many simplifying assumptions and the actual Cassini mission trajectory depicted in Fig. 6 most likely resulted from a more sophisticated set of objectives and constraints than the simple ΔV minimization performed by MDTOP for the analysis conducted in this study. The MDTOP solution uses significantly less C_3 than the actual Cassini trajectory, which as a consequence, requires some of the gravity assists to be powered. To obtain a trajectory that more closely matches the actual Cassini trajectory for the purposes of comparison, the higher accuracy JPL DE405 planetary ephemeris is used, and the objective function is changed to maximum payload, assuming a simple spacecraft propulsion model. An engine specific impulse of 328 s and a structural factor of 0.15 are used for the spacecraft, which is launched from a Boeing Delta IV Heavy [14]. As seen in Table 1, given the

Table 1 Comparison of MDTOP results and the published data for Cassini

Trajectory	Launch	Venus GA I	DSM	Venus GA II	Earth GA	Jupiter GA	Saturn arrival
Cassini	10/15/1997	4/26/1998	12/3/1998	6/24/1999	8/18/1999	12/30/2000	7/1/2004
(actual trajectory)	$C_3 = 16.6$ km^2/s^2	0 m/s	450 m/s	0 m/s	0 m/s	0 m/s	633 m/s
MDTOP	10/21/1997	4/30/1998	11/30/1998	6/26/1999	8/18/1999	1/13/2001	10/19/2004
(max payload, DE405)	$C_3 = 15.93$ km^2/s^2	0 m/s	428.5 m/s	0 m/s	0 m/s	0 m/s	556.5 m/s
MDTOP	11/2/1997	4/24/1998	1/23/1999	6/27/1999	8/18/1999	1/16/2001	10/31/2004
(min ΔV, static ephemeris)	$C_3 = 10.49$ km^2/s^2	303.5 m/s	271.5 m/s	0 m/s	518.9 m/s	0 m/s	555.9 m/s

Table 2 Run time in minutes required to reliably optimize the Cassini mission profile

F	$CR = 0.4$	$CR = 0.6$	$CR = 0.8$
$NP = 20$			
0.2	23.160	No solution	No solution
0.4	3.718	3.308	No solution
0.6	19.139	2.759	1.422
0.8	160.157	3.028	1.427
1.0	267.293	109.624	No solution
rand[−1, 1]	4.872	2.400	1.403
$NP = 28$			
0.2	24.086	2.421	No solution
0.4	5.829	3.136	3.973
0.6	102.410	5.213	1.049
0.8	193.022	13.353	2.512
1.0	265.514	386.562	43.971
rand[−1, 1]	11.460	3.575	1.201
$NP = 36$			
0.2	14.327	354.140	49.879
0.4	13.075	5.404	1.841
0.6	195.502	9.052	1.764
0.8	No solution	206.790	3.030
1.0	No solution	631.483	24.231
rand[−1, 1]	9.340	2.100	1.278

more detailed ephemeris and objective function, MDTOP is capable of reproducing the Cassini trajectory very closely, though some differences exist due to slightly different end conditions and mission duration.

Table 2 shows the $T_{95\%}$ values for the optimization of the Cassini mission over the range of optimization tuning parameters considered. The minimum ΔV solution obtained by MDTOP for the Cassini trajectory profile has a total ΔV of 4.867 km/s, and all solutions with a total ΔV less than 4.900 km/s are considered to belong to the best solution. As seen in Table 2, the tuning parameters have a very large effect on the success of DE. Whereas some setups optimize the problem in a little over 1 min, others take hundreds of minutes or never obtain the minimum ΔV solution.

The six best optimization parameter sets found for Cassini are detailed in Table 3, where the hyphens denote that the combination was not considered. The best optimization parameter sets were found to all have a crossover probability of 0.8, which allows for the removal of crossover probability as a variable in the subsequent case studies. Of the best six parameter sets, it is found that the highest probability of finding the global optimum is 19.5% and the shortest time required to find it reliably is 1.05 min. The histogram associated with the lowest $T_{95\%}$ time is included as Fig. 8. As seen in that histogram, even the best set of optimization parameters for the Cassini mission results in a low occurrence of the minimum ΔV solution, with a frequency of 18.9%. However, due to the fast

Table 3 Performance of the best six tuning parameters on the Cassini mission profile

F	$NP = 20$	$NP = 28$	$NP = 36$
Frequency of best solution, %			
0.6	16.1	18.9	——
0.8	19.5	——	——
rand[−1, 1]	7.2	13.9	17.1
Run time per trial, s			
0.6	5	4.4	——
0.8	6.2	——	——
rand[−1, 1]	2.1	3.6	4.8
95% confidence time, min			
0.6	1.422	1.049	——
0.8	1.427	——	——
rand[−1, 1]	1.403	1.201	1.278

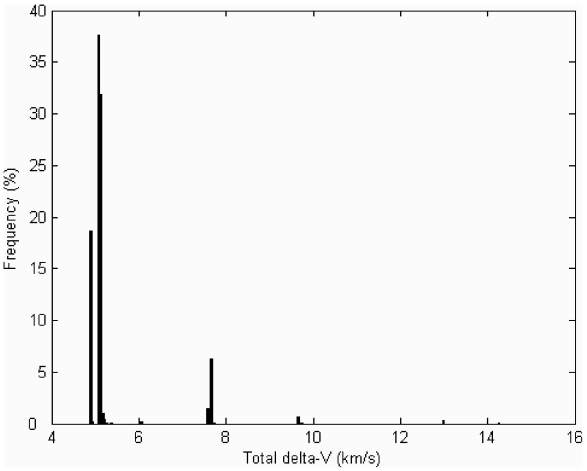

Fig. 8 Cassini solution histogram associated with the best optimization parameter set.

operation of MDTOP, 4.4 s per trial in this case, and its independence from user interaction, the global minimum can be found with repetitive trials in only 1.05 min, with a probability of 95%. As a side note, the DE tuning parameters used in the University of Reading study find a minimum ΔV with MDTOP of 4.891 km/s on the Cassini mission and a $T_{95\%}$ time of 22.1 h. The tuning parameters from the University of Glasgow study, when used with MDTOP, result in a minimum ΔV of 4.959 km/s which is outside the range of the best known solution. Better DE tuning parameters are a possible explanation for the somewhat better performance of DE in the Reading study as compared to the Glasgow study.

Galileo Case Study

Another example used to gauge this method's capabilities is the 1989 Galileo mission to Jupiter, which is reproduced in Fig. 9 from [15]. Nine design variables are involved: launch date, five times of flight, and three variables to define the position of the DSM. The Galileo mission is optimized by MDTOP with the following bounds and assumptions. The launch date can occur any time in 1989. The total time of flight is constrained to be less than 6.1 years to coincide with the time of flight of the Galileo mission, as longer times of flight result in a lower total mission ΔV. The close encounters of the small bodies Ida and Gaspra are ignored as those events were selected out of convenience after the baseline mission was chosen [16]. One deep space maneuver is used between the two Earth gravity assists. Finally, the spacecraft enters into an orbit about Jupiter with a parking orbit size of 4×299 Jupiter radii as was specified for the reference orbit. The plane of the Jupiter arrival orbit is undefined for this investigation.

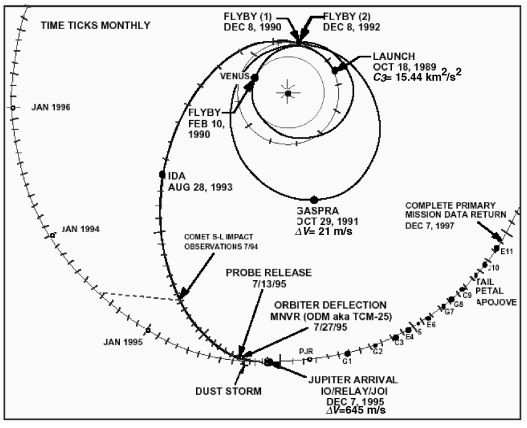

Fig. 9 Published Galileo spacecraft trajectory [15].

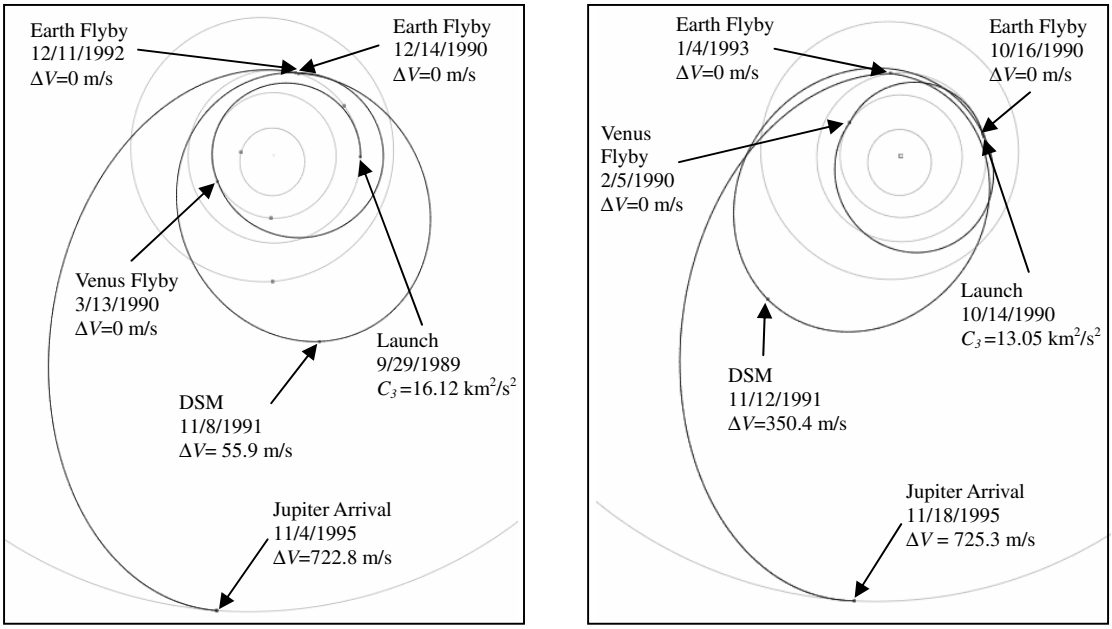

Fig. 10 Two solutions for the Galileo mission profile: a) local minimum, b) minimum ΔV.

The MDTOP trajectory shown in Fig. 10a corresponds very closely with the actual Galileo trajectory. For the ΔV minimization of the Galileo flyby sequence, this Galileo-type trajectory was only a local minimum. A lower ΔV solution found with MDTOP, which requires approximately 150 m/s less ΔV, is shown in Fig. 10b and is compared with the actual Galileo trajectory in Table 4.

The minimum ΔV trajectory requires less C_3 from the high efficiency launch vehicle and more ΔV for the DSM which is performed with lower efficiency spacecraft engines. Therefore, if a spacecraft system model was incorporated into the objective function, it would be expected that a Galileo-type trajectory would be superior. For this analysis, an engine specific impulse of 328 s and a structural factor of 0.15 are used for the spacecraft, which is launched from a Boeing Delta IV Heavy. The maximum payload mass trajectory obtained by MDTOP is indeed more similar to the actual Galileo trajectory than the minimum ΔV solution.

To determine which set of parameters is the best for the widest array of missions, the best six tuning parameter sets from the Cassini analysis are further compared on the Galileo mission. The performance of the optimization parameters is presented in Table 5. The highest occurrence of finding the presumed global minimum is 19.1%, while the shortest $T_{95\%}$ run time is 0.844 min. Figure 11 shows the histogram associated with the highest performing tuning parameter set. Also noted in Fig. 11 are the peaks associated with the Galileo-type trajectory, seen in Fig. 10a, and the minimum ΔV trajectory, seen in Fig. 10b. The best solution obtained for the Galileo mission has a total ΔV of 4.637 km/s. All trajectories with a total ΔV less than 4.720 km/s were considered to belong to the best solution after an investigation of the solution space. All of the top six tuning parameter sets for the Cassini trajectory profile also result in low $T_{95\%}$ run times for the Galileo case study.

Tempel 1 Comet Surface Sample Return Case Study

The next example used to investigate the selection of the DE tuning parameters is a hypothetical surface sample return mission to comet Tempel 1. Fourteen design variables are required to characterize this mission: launch date, six times of flight, stay duration, and six variables to define the positions of the two DSMs. The spacecraft is allowed to depart from Earth any time in 2008. An

Table 5 Performance of the best six tuning parameters on the Galileo mission profile

F	$NP = 20$	$NP = 28$	$NP = 36$
Frequency of best solution, %			
0.6	11.3	11.3	——
0.8	4.8	——	——
rand[−1, 1]	9.3	12.2	19.1
Run time per trial, s			
0.6	2.6	4.0	——
0.8	2.6	——	——
rand[−1, 1]	2.4	2.2	5.4
95% confidence time, min			
0.6	1.083	1.666	——
0.8	2.639	——	——
rand[−1, 1]	1.228	0.844	1.272

Table 4 Comparison of MDTOP results and the published data for Galileo

Trajectory	Launch	Venus flyby	Earth flyby I	DSM	Earth flyby II	Jupiter arrival
Galileo	10/18/1989	2/10/1990	12/8/1990	10/29/1991	12/8/1992	12/7/1995
(actual trajectory)	$C_3 = 15.44$ km^2/s^2	0 m/s	0 m/s	21 m/s	0 m/s	645 m/s
MDTOP	11/6/1989	2/20/1990	12/10/1990	12/22/1991	12/6/1992	12/12/1995
(max payload, DE405)	$C_3 = 13.41$ km^2/s^2	0 m/s	0 m/s	96.9 m/s	0 m/s	809.0 m/s
MDTOP Fig. 10a	9/29/1989	3/13/1990	12/14/1990	11/8/1991	12/11/1992	11/4/1995
(local ΔV, static ephemeris)	$C_3 = 16.12$ km^2/s^2	0 m/s	0 m/s	55.9 m/s	0 m/s	722.8 m/s
MDTOP Fig. 10b	10/14/1990	2/5/1990	10/16/1990	11/12/1991	1/4/1993	11/18/1995
(min ΔV, static ephemeris)	$C_3 = 13.05$ km^2/s^2	0 m/s	0 m/s	350.4 m/s	0 m/s	725.3 m/s

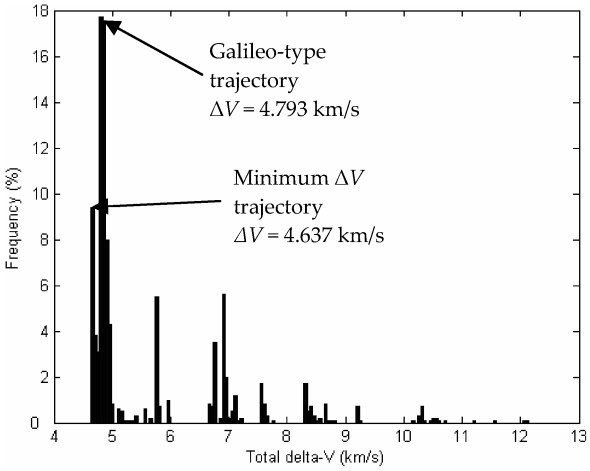

Fig. 11 Galileo solution histogram associated with the best optimization parameter set.

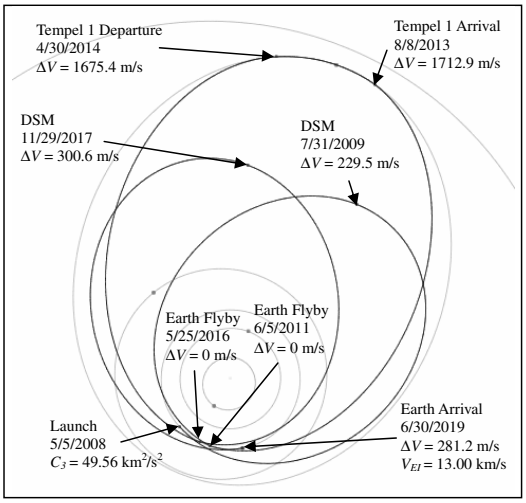

Fig. 12 Optimized round-trip mission to Tempel 1.

Earth gravity assist and one DSM are used on the way to the comet. The comet is assumed to be massless and the stay time is constrained to lie between 60 and 600 days. An Earth gravity assist and a DSM are used for the return trip to Earth, where the reentry speed is limited to 13.0 km/s. The total mission duration is constrained to be less than 12 years. Figure 12 shows the minimum ΔV solution obtained by MDTOP.

Although there are no published data available to determine the accuracy or optimality of the trajectory shown in Fig. 12, this example still allows for further comparison of the six optimization parameter sets. The best solution obtained has a total ΔV of 11.21 km/s, and all solutions with a total ΔV less than 11.50 km/s are considered to belong to the best solution. The results collected in Table 6 show that the Tempel 1 mission is slightly easier to optimize than the Cassini or Galileo missions, with the minimum $T_{95\%}$ time being only 0.452 min. This ease of optimization is most likely attributed to the lack of high performing suboptimal local minima. The histogram corresponding to the most effective parameter set ($NP = 20$, $CR = 0.8$, $F = 0.6$), in Fig. 13, shows the minimum ΔV solution being found nearly 4 times more frequently than any other solution. On this mission profile, DE does not have the misconvergence problems observed in the histograms of the Cassini and Galileo solutions, where high performing suboptimal minima are found most of the time.

Table 6 Performance of the best tuning parameters on a round-trip mission to Tempel 1

F	$NP = 20$	$NP = 28$	$NP = 36$
Frequency of best solution, %			
0.6	26.6	40.0	——
0.8	13.9	——	——
rand[−1, 1]	8.4	19.3	32.7
Run time per trial, s			
0.6	2.8	5.0	——
0.8	5.0	——	——
rand[−1, 1]	2.8	3.3	6.5
95% confidence time, min			
0.6	0.452	0.489	——
0.8	1.668	——	——
rand[−1, 1]	1.603	0.768	0.819

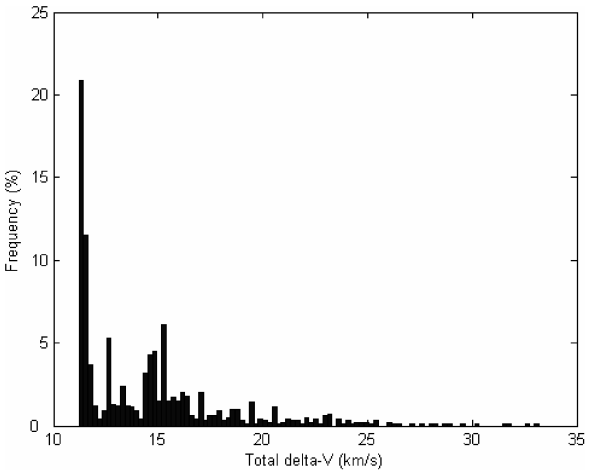

Fig. 13 Tempel 1 solution histogram associated with the best optimization parameter set.

Crewed Mars Mission Case Study

The capability to optimize planetary operations as part of an overall round-trip mission is one of the strengths associated with using a powerful global optimization routine like differential evolution. The 2030 Mars conjunction trajectory shown in Fig. 14 is the result of optimizing a crewed mission to Mars which uses orbital rendezvous and parking orbits previously described. This problem is parameterized by seven design variables: launch date, two times of flight, stay duration, landing site latitude, and the eccentricity and periapsis altitude of the parking orbit. For this case, the launch date is constrained to be no more than 1000 days after 1 January 2030. The stay duration at Mars must be between 60 and 600 days, while the

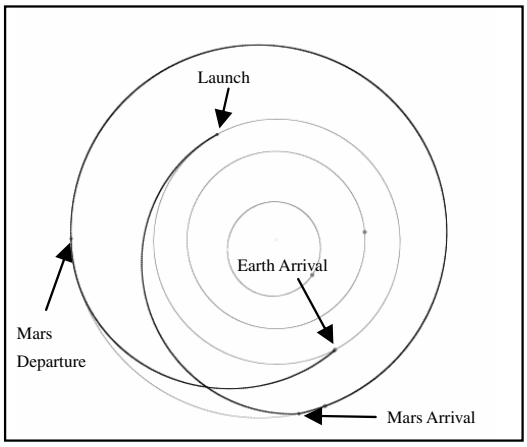

Fig. 14 Optimized round-trip 2031 crewed Mars mission with orbital rendezvous.

Table 7 Details of round-trip crewed Mars mission with optimized orbital rendezvous

Launch	Mars arrival	Arrival parking orbit	Descent
1/14/2031	8/12/2031	$a = 6186.5$ km	Landing latitude = 70.05 deg
$C_3 = 10.69$ km^2/s^2	$\Delta V = 3483$ m/s	$e = 0.000006$	Lighting angle = 5.00 deg
	$\boldsymbol{V}_\infty = [3.848, -2.884, 0.648]$	$i = 70.66$ deg	$\Delta V = 416.6$ m/s
	(km/s, Mars frame)	$\Omega = 145.86$ deg	
		$\omega = 95.00$ deg	
Stay duration = 492.50 days			
Ascent	Precessed parking orbit	Mars departure	Earth reentry
$\Delta V = 4375$ m/s	$a = 6186.5$ km	12/17/2032	7/15/2033
	$e = 0.000006$	$\Delta V = 2070$ m/s	$V_{\mathrm{EI}} = 13.00$ km/s
	$i = 70.66$ deg	$\boldsymbol{V}_\infty = [-2.639, -1.116, 0.214]$	$\Delta V = 531.8$ m/s
	$\Omega = 201.42$ deg	(km/s, Mars frame)	
	$\Omega = 247.39$ deg		

Table 8 Performance of best tuning parameters on round-trip Mars mission

F	$NP = 20$	$NP = 28$	$NP = 36$
Frequency of best solution, %			
0.6	7.4	14.5	——
0.8	13.8	——	——
rand[−1, 1]	4.8	12.9	24.1
Run time per trial, s			
0.6	0.50	0.76	——
0.8	0.51	——	——
rand[−1, 1]	0.50	0.84	0.86
95% confidence time, min			
0.6	0.325	0.242	——
0.8	0.171	——	——
rand[−1, 1]	0.508	0.304	0.156

total mission time is limited to 2.5 years. This is assumed to be a crewed mission, so there is an additional constraint on the maximum flight time between Earth and Mars of 210 days. The landing site at Mars is arbitrarily constrained to lie between 70 and 90° latitude. The parking orbit periapsis must have an altitude between 300 and 3000 km. The maximum period of the orbit is set at 24 h. The lighting angle required for visibility during descent through the atmosphere to the landing site is constrained to lie between 5 and 25 deg. The details associated with the optimum trajectory that satisfies these constraints while ensuring a minimum-energy, in-plane descent from apoapsis, in-plane ascent, and tangential periapsis burns at arrival and departure are listed in Table 7. The best solution found for this mission has a total ΔV of 14.1467 km/s. All solutions with a total ΔV less than 14.15 km/s are determined to belong to the best solution.

Despite the number of constraints imposed on this problem, it was the easiest mission to optimize out of the four that were investigated.

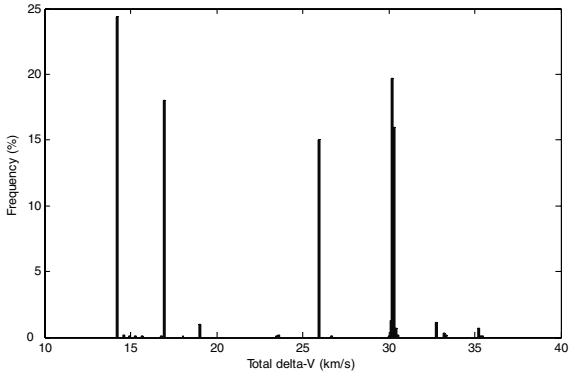

Fig. 15 Mars solution histogram associated with the best tuning parameter set.

Table 8 shows the performance obtained with the six best tuning parameter sets. The best $T_{95\%}$ run time of 0.156 min is obtained by the set ($NP = 36$, $CR = 0.8$, $F = \mathrm{rand}[-1, 1]$). The solution histogram for this set of DE parameters is shown in Fig. 15. The relatively large frequency of high ΔV solutions most likely results from the discrete nature of the parking orbit alignment constraint. For this case, the best solution is the most commonly found, with a frequency of 24.1%.

To determine the best overall set of optimization parameters for the four missions investigated, the $T_{95\%}$ time is averaged over all four missions, with the results shown in Table 9. By using an average value, the more time consuming missions are weighted more heavily, which is desirable, given that the focus of this method is on optimizing complicated trajectories. The set that results in the minimum average $T_{95\%}$ is found to be ($NP = 28$, $CR = 0.8$, $F = \mathrm{rand}[-1, 1]$), which was also found to be the best setting for optimizing the Galileo mission. The maximum $T_{95\%}$ time required to reliably optimize any of the four test cases with ($NP = 28$, $CR = 0.8$, $F = \mathrm{rand}[-1, 1]$) is only 1.2 min, occurring for the Cassini mission analysis.

Conclusions

The combination of a fast, zero sphere-of-influence based solar system model and a powerful global stochastic optimization routine, differential evolution, yields a preliminary trajectory optimization tool that can quickly locate the best solution to complex multiple gravity-assist missions. Highly constrained round-trip missions with parking orbits can be optimized from end to end. Alternative flyby sequences and launch windows can be quickly investigated, as the time required to optimize a single mission scenario is often less than a minute, and no specific detailed knowledge of the design space is required before beginning a run.

The performance of differential evolution was found to be highly sensitive to the selection of the global optimization routine's tuning parameters. The basic tuning parameters for the stochastic search

Table 9 Average performance of tuning parameters on all four test cases

F	$NP = 20$	$NP = 28$	$NP = 36$
Avg. frequency of best solution, %			
0.6	15.4	21.2	——
0.8	13.0	——	——
rand[−1, 1]	7.4	14.6	23.3
Avg. run time per trial, s			
0.6	2.7	3.5	——
0.8	3.6	——	——
rand[−1, 1]	2.0	2.5	4.4
Avg. 95% confidence time, min			
0.6	0.820	0.861	——
0.8	1.476	——	——
rand[−1, 1]	1.185	0.779	0.881

method are the population size, crossover probability, and the mutation scaling factor. By comparing various tuning parameter combinations for a variety of complex interplanetary mission scenarios, a set of tuning parameters ($NP = 28$, $CR = 0.8$, $F = \text{rand}[-1, 1]$) was identified as being superior for solving general interplanetary trajectory problems. This set performed well for all four trajectory test cases, globally optimizing the Cassini mission using a 3.0 GHz Pentium 4 processor in a run time of 1.2 min with a confidence level of 95%. This set also optimized the Galileo mission in only 51 s with a confidence level of 95%. In this study, lower-accuracy static ephemerides were used to reduce the computational time necessary to generate the multiple 1000 trial samples required to conduct the comparative analyses. The use of a high-accuracy DE405 ephemeris results in run times that are approximately double those cited here.

This investigation, while not exhaustive, has shown that the best differential evolution tuning parameters do not follow any clearly identifiable pattern. On the other hand, multiple tuning parameter sets have been identified that perform well on each of the four diverse test problems. These two observations suggest that a probabilistic assessment of the tuning parameters on a representative set of test problems is both necessary and adequate to maximize the performance of the differential evolution algorithm for a general high-thrust trajectory design problem.

Acknowledgment

The work described in this paper was funded in whole or in part by the In-Space Propulsion Technology Program, which is managed by the NASA Science Mission Directorate in Washington, D.C., and implemented by the In-Space Propulsion Technology Projects Office at Marshall Space Flight Center in Huntsville, Alabama.

References

[1] Hartman, J. W., Coverstone-Carroll, V. L., and Williams, S. N., "Optimal Interplanetary Spacecraft Trajectories via Pareto Genetic Algorithm," *Journal of the Astronautical Sciences*, Vol. 46, No. 3, 1998, pp. 267–282.

[2] Crain, T., Bishop, R. H., Fowler, W., and Rock, K., "Interplanetary Flyby Mission Optimization Using a Hybrid Global-Local Search Method," *Journal of Spacecraft and Rockets*, Vol. 37, No. 4, 2000, pp. 468–474.

[3] Vasile, M., and De Pascale, P., "Preliminary Design of Multiple Gravity-Assist Trajectories," *Journal of Spacecraft and Rockets*, Vol. 43, No. 4, 2006, pp. 794–805.

[4] Bessette, C. R., and Spencer, D. B., "Optimal Space Trajectory Design: A Heuristic-Based Approach," AAS Paper 06-197, Jan. 2006.

[5] Myatt, D. R., Becerra, V. M., Nasuto, S. J., and Bishop, J. M., "Advanced Global Optimization Tools for Mission Analysis and Design," Final Report of ESA Ariadna ITT AO4532/18138/04/NL/MV, Call 03/4101, 2004.

[6] Di Lizia, P., and Radice, G., "Advanced Global Optimization Tools for Mission Analysis and Design," Final Report of ESA Ariadna ITT AO4532/18139/04/NL/MV, Call 03/4101, 2004.

[7] Olds, A. D., "Interplanetary Trajectory Optimization with Differential Evolution," M.S. Thesis, Univ. of Missouri–Columbia, Columbia, MO, Dec. 2005.

[8] Bate, R. R., Mueller, D. D., and White, J. E., *Fundamentals of Astrodynamics*, Dover Publications, New York, 1971.

[9] Hale, F. J., *Introduction to Space Flight*, Prentice–Hall, Upper Saddle River, NJ, 1994.

[10] Desai, P. N., Braun, R. D., and Powell, R. W., "Aspects of Parking Orbit Selection in a Manned Mars Mission," NASA Technical Paper 3256, Dec. 1992.

[11] Desai, P. N., and Buglia, J. J., "Arrival and Departure Impulsive ΔV Determination for Precessing Mars Parking Orbits," *Journal of the Astronautical Sciences*, Vol. 41, No. 1, 1993, pp. 1–18.

[12] Storn, R., and Price, K., "Differential Evolution—A Simple and Efficient Heuristic for Global Optimization over Continuous Spaces," *Journal of Global Optimization*, Vol. 11, No. 4, Dec. 1997, pp. 341–359.

[13] *Cassini Mission Plan*, JPL Publication D-5564, Rev. N, May 2002.

[14] *Delta IV Payload Planners Guide*, Boeing, Oct. 2000.

[15] *Galileo, The Tour Guide* (and a summary of the mission to date), edited by Jean H. Aichele, JPL Publication D-13554, June 1996.

[16] D'Amario, L. A., Byrnes, D. V., Johannesen, J. R., and Nolan, B. D. "Galileo 1989 VEEGA Trajectory Design," *Journal of the Astronautical Sciences*, Vol. 37, No. 3, 1989, pp. 281–306.

B. Marchand
Associate Editor